

PAST, PRESENT, AND FUTURE STRESS-INTENSITY FACTOR SOLUTIONS FOR CRACKS AT HOLES

James C. Sobotka¹, R. Craig McClung², Yi-Der Lee², and Joseph W. Cardinal²

¹ Southwest Research Institute® (SwRI®), USA, james.sobotka@swri.org

² Southwest Research Institute (SwRI), USA

Abstract: This document summarizes advances in stress-intensity factor (SIF) solutions for cracks at holes, set in the historical context of the past forty years and current problems that demand new, novel solutions to support damage tolerance (DT) assessments. Special attention is given to corner cracks since they are usually the initial crack state and often dominate total DT lifetime.

Classic solutions by Newman and Raju (1980s) and Fawaz and Andersson (2000s) supported wide plates, requiring separate finite-width correction factors for practical applications. While the Newman-Raju correction factors were state of the art for their time, they have significant limitations. Our recent developments feature new equations with improved accuracy for tension, bend, and pin-loading for single or dissimilar double cracks. Post-transition scenarios led us to develop novel compounding solutions for corner-through or dissimilar through-through crack combinations, building on formulations from NRC-Canada (late 2000s).

Weight function (WF) solutions address the practical challenge of finite-geometry effects in a different way. Our WF formulation employs analytical basis functions coupled with large matrices of reference solutions over the range of finite widths and offsets. More importantly, the WF approach handles additional stress states besides uniform remote loading and permits explicit treatment of residual stress, including shakedown residual stress from local plasticity. Most WF solutions are based on stress gradients in a single direction, but because stresses at the corner of a hole are inherently bivariant, we have also developed a WF solution that accommodates stress gradients varying in all directions on the crack plane of a corner (or a surface) crack.

Current DT challenges involve physical issues that may not be tractable using conventional approaches. These challenges include cold expansion, interference/clearance fits, manufacturing-induced residual stress, nonlinear material response, out-of-plane bending, multi-hole interaction, and multi-crack interaction that could be characterized as multi-site damage. Our recent efforts exploit advances in curved through-crack descriptions, principal component analysis, automatic generation of crack fronts for finite element analyses, and machine learning via Gaussian Process models. These tools are leading to incremental advances to support cracks at a row of holes, interference fit for through cracks, and tractable calculations of bivariant stresses near stress concentrators under remote loading.

Keywords: Stress-Intensity Factor Development; Damage tolerance; Weight function; Corner crack

INTRODUCTION

Circular holes, rows of holes, small holes next to large holes, and rows and columns of holes are ubiquitous in airframes. The hole geometry itself elevates stresses above the baseline stresses in the surrounding material. Manufacturing a hole can introduce defects that may not be eliminated by additional operations. Further complicating matters, holes often carry pins, bolts, rivets, and other fasteners that induce nonlinear local stresses from contact that contributes to fatigue crack formation from various processes, *e.g.*, wear or corrosion. These features promote the initiation and growth of fatigue cracks under cyclic loading histories. If these cracks fracture, it may jeopardize structural integrity, *i.e.*, holes in an airframe often represent fatigue-critical locations. Consequently, certification authorities require damage tolerance (DT) analyses at many holes in an airframe.

Practical stress-intensity factor (SIF) solutions are needed to support these DT assessments. Here, we distinguish a practical solution from a higher-fidelity solution. The practical solution will be applied at potentially thousands of locations in an aircraft and may need to incorporate possible variations in the loading spectrum, material, environment, and initial crack state. Consequently, the practical solution must be fast, robust, physically-realistic, and accurate if a bit on the conservative side. These considerations do not apply for a higher-fidelity, multi-point fracture assessment based on 3D finite element analyses that will typically be focused at a location with less uncertainty.

Of the practical SIF solutions at holes, corner cracks take priority over surface cracks, through cracks, and embedded cracks. Practical DT assessments idealize the corner crack as a quarter-elliptical crack front placed at the intersection of the hole and free surface. Corner cracks are often taken as the small initial crack in a DT assessment, and the bulk of fatigue crack growth (FCG) life at a hole happens in the corner crack configuration as a result. Similar analyses with an initial surface crack centered in the bore or an initial embedded crack would result in much longer lives relative to a corner crack. An initial through crack would need to be so small as to be physically unrealistic. Initial cracks set as corner cracks balance physical reality (initial cracks are small) and conservatism (they grow quickly).

Here, we focus on the development of practical SIF solutions for corner cracks at circular holes over the past forty years. During that time frame, a variety of solutions have appeared in the open literature and in proprietary DT tools. Different solutions support different sets of geometric bounds, enable different loading capabilities, have different formulations, and feature different levels of accuracy. Consequently, an analyst working with, for example, the fracture and FCG software NASGRO® [1] can select from eight SIF solutions for various combinations of a corner crack at a round hole in a plate: CC08 (univariant weight function (WF)), CC10 (early generation bivariant WF), CC26 (later generation WF), CC15 (adds a broken ligament), CC16 (data-table look-up), CC17 (two unequal corner cracks), CC24 (a row of holes), and CC25 (countersunk hole). Additionally, there are two solutions for a corner crack in a lug (CC19 and CC23), one hybrid solution for a corner crack and through crack (HC01), and four legacy superseded solutions for similar geometries (CC02, CC03, CC04, and CC07).

The proliferation of SIF solutions for similar or even identical geometries causes confusion for analysts, developers, and certifying authorities. As is often the case, the various SIF solutions reflect a historical development whereby the capabilities, accuracy, and speed of earlier solutions are refined by later solutions. As a result, this paper approaches the various SIF solutions from a similar historical perspective. First, we review classical approaches to this problem that rely on large data tables of cracks at holes in wide plates and the accompanying finite-width correction factors. We detail issues that have resulted from this formulation and their resolution. Second, we discuss weight function (WF) approaches to the problem that support arbitrary stress gradients and permit wider capabilities. The next section demonstrates and discusses the variability of nominally identical life predictions made using the different solutions. Afterwards, we review corner crack SIF solutions near round holes that feature some deviation from the standard geometry, *e.g.*, a countersunk hole. We then review some recent innovations in the practical development of SIF solutions. Finally, this document finishes with a review of future avenues of research and development.

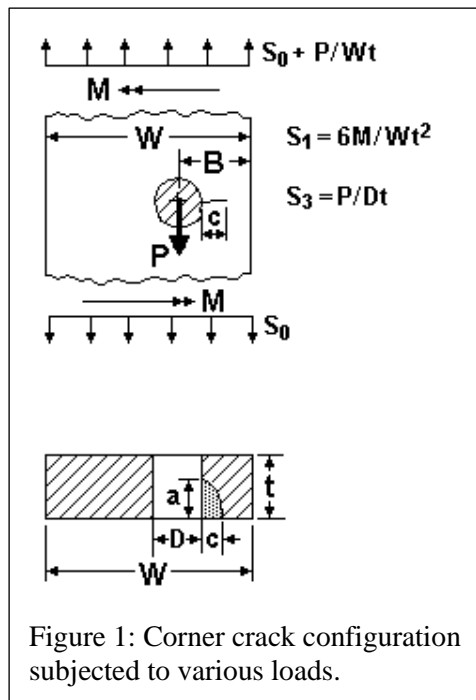


Figure 1: Corner crack configuration subjected to various loads.

CLASSIC SIF SOLUTIONS

This section focuses on two classical solutions: the Newman-Raju (NR) solutions [2] and the Fawaz-Andersson (FA) solutions [3]. These solutions approach the problem using similar methods: Develop a SIF solutions for wide plates and apply independent finite-width correction factors to address finite-width plates with offset holes that reflect real geometries. The original finite-width correction factors have been shown to be flawed for certain geometries and require revisions as discussed in this section. Figure 1 shows the basic geometry used in these analyses.

Newman-Raju Solutions

In 1979, Raju and Newman [3] developed quarter-symmetric finite element models of two identical corner-cracks at a hole in a plate. SIF values from these geometries could then be converted to a single corner crack at hole using the Shah correction factor [4]. This approach enabled analyses that varied crack shape ($a/c = 0.2, 1, 2$), size ($a/t = 0.2, 0.5, 0.8$), and hole thickness ($D/2t = 0.5, 1$) for wide plates with remote loading. Raju and Newman performed 18 total analyses with some geometries having up to 9300 degrees of freedom. These solutions included remote tension (S_0), remote in-plane bending (S_1), and a wedge loading that could (with some assumptions) be converted into a pin loading (S_3).

These analyses center the hole in a very wide plate. This approach prevents the direct applicability of these solutions to real geometries with finite-sized holes ($D/2B \geq \approx 10\% - 20\%$) and holes that are offset in the geometry. Consequently, Newman and Raju developed a set of finite-width and offset correction factors [5]. Furthermore, these papers include a series of closed form (empirical) expressions that permit users to determine SIF values at cracks not included in the original (very) sparse matrix. The NR solutions have been extensively used in design and analysis since their original release. In recent versions of NASGRO, they form the basis for CC02, which is now categorized as a superseded solution. Despite the primitive computational capabilities in their development, the NR solutions have decent accuracy for most applications and have been used successfully for many years to perform DT analyses on many practical structures.

Fawaz-Andersson Solutions

The FA solutions [3] provide the next set of landmark solutions. Computational capabilities increased by nearly 400X in the 25 years between the NR solutions and the FA solutions. The FA database features 7150 combinations of $D/2t$, a/t , and a/c (vs. 18 solutions for NR). Each solution represents the result from the *hp*-version of the finite element method to achieve an exponential convergence of the SIF value along the crack front. The authors extend the numerical results with a splitting approach that permits them to solve for the SIF solutions of two unequal corner cracks at a hole, and this second database has 226,875 SIF solutions. Results shown by FA demonstrate the fidelity of the NR solutions for some cases and indicate problems (perhaps due to extrapolation) with other cases. In NASGRO, the FA results are the basis for CC16 (single crack at a hole) and CC17 (two unequal cracks at a hole).

Recent Modifications

It has been recognized for some time that the original NR solutions required some updating [6]. Consequently, Newman released an updated version of the NR equations more suitable for deep cracks [7]. It is less well known that the finite-width correction factors ($F_{W,i}$) and offset correction factors ($F_{O,i}$)

require some fine-tuning to align the SIF values for wide plates with the SIF values for finite-width geometries. In both the NR and FA solutions (described as geometry correction factors β_i), the resolved SIF value can be computed as shown in Eqn. 1 using the three loading components $i = 0,1,3$:

$$SIF = \sum_{i=0,1,3} F_{W,i} \times F_{O,i} \times \beta_i \times S_i \sqrt{\pi a}. \quad (1)$$

Detailed analyses of single corner cracks at holes in finite-width plates revealed issues for certain crack configurations. As a result, more accurate solutions for $F_{W,i}$ and $F_{O,i}$ have been developed. Guo determined simple corrections to $F_{W,i}$ for remote tension and bend [1]. Sobotka considered pin-loading and found that $F_{W,i}$ and $F_{O,i}$ needed to be combined into a single function. He constructed this function by interpolating over results from a large database of solutions derived from WF SIFs. Figure 2 shows the improvement in the finite-width correction factor using the approach outlined by Guo.

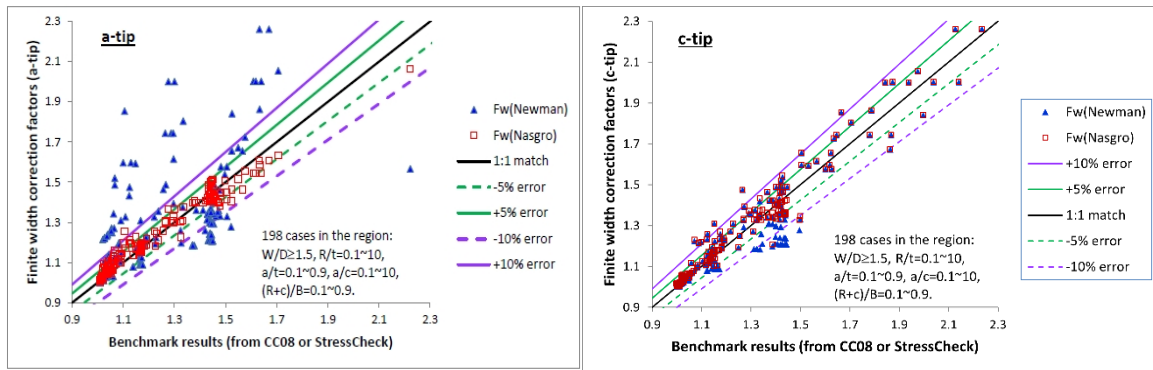


Figure 2: Old and new finite-width correction factors for the a-tip and c-tip under S_0 loading.

MODERN WEIGHT FUNCTION SOLUTIONS

Besides the issues highlighted in the previous section, both the NR and FA solutions suffer from several restrictions that motivated subsequent developments:

- Limited to ideal scenarios of uniform tension, out-of-plane bending, and pin loading;
- Cannot support high-load levels that would trigger yielding localized near the hole;
- Do not support local residual stresses, *e.g.*, from cold expansion.

These capabilities are particularly important for practical structural analysis of cracks in complex stress fields. Weight function (WF) solutions provide an alternative approach to the curve fits and data tables generated in the earlier efforts. WF solutions enable analysts to determine SIF values for arbitrary stress fields, including the stress fields in the earlier bullets. Furthermore, the WF solutions have been shown to be extremely robust and require fewer analyses for calibration than classical data table solutions. Consult Wu [8] for a comprehensive review of recent WF approaches.

Theory

WF solutions were originally developed by Bueckner [9] and Rice [10]. Specifically, these researchers determined that the SIF of one cracked body under some loading was related to the SIF of the same cracked body under a different loading. Here, the transfer function from the first SIF (with displacement field u_i^{1st}) to the second SIF depends on (1) $\partial u_i^{1st} / \partial a$, where a is the crack length and (2) the tractions (excluding body forces) needed to close the crack face under the second loading condition. This result is derived from energy arguments and applies to any crack in a linear-elastic material. Traction may be determined based on the stresses in the uncracked body, and, as a result, WFs are typically valid only if

the crack does not trigger load redistribution. Besides this restriction, the WF approach is extremely general and has been applied to a wide variety of geometries, loadings, and other configurations.

One useful way to define WF solutions is to distinguish between univariant WFs and bivariant WFs. Univariant WFs enable the stress to vary in one direction that is often referred to as the primary stress direction. Bivariant WFs enable the stress to vary across the full 2D crack plane. For cracks near a hole, bivariant WFs may be needed if stress gradients vary strongly through the thickness, *i.e.*, thick plates.

The general form of a univariant WF solution ($w(x, a)$) may be expressed as follows in Eqn. (2):

$$SIF = \int_0^a \sigma(x) w(x, a) dx. \quad (2)$$

In this expression, a is a measure of crack length or depth, and $\sigma(x)$ denotes the stress component normal to the crack surface derived from the uncracked body and varying along the primary direction of crack extension x . Eqn. (2) indicates that the SIF is found by integrating the stress in the uncracked body over the “shadow” of the crack front. The stress gradient is arbitrary. It can include contributions from remote loads, yielding, and residual stresses. The stress gradient may be written as a closed-form expression, a combination of polynomials (or other functions), or as a table of stress-distance pairs. A bivariant WF solution extends the weight function to consider stress variations in both the primary and secondary directions. It is integrated over the area of the crack front. Quadrature of the area integral requires additional computational effort.

Implementation

Our efforts have shown that the generalized WF proposed by Shen and Glinka [11] provides a reasonable approach to develop univariant WFs as shown in Eqn. (3):

$$w(x, a) = \frac{2}{\sqrt{2\pi(a-x)}} \left[1 + M_1 \left(1 - \frac{x}{a}\right)^{\frac{1}{2}} + M_2 \left(1 - \frac{x}{a}\right) + M_3 \left(1 - \frac{x}{a}\right)^{\frac{3}{2}} \right]. \quad (3)$$

Here, M_1 , M_2 , and M_3 represent parameters dependent on the particular crack geometry of interest. They are usually determined from reference SIF values computed by finite element analyses. The reference parameters are determined at several crack plane loading conditions. The physical basis of the underlying WF formulation stabilizes the interpolation of reference solutions and enables analysts to calibrate the WF using many fewer solutions than needed for the FA database. Such effectiveness can be shown by comparing the 7150 solutions in the FA database that only supports wide plates vs. the univariant WF solution in NASGRO (CC08) that only uses 1674 solutions to calibrate the WF solution that considers finite-width plates and offset holes for an extensive range of geometries.

Bivariant WF solutions are more sophisticated than the expression shown in Eqn. (3). As documented by Lee [12], a bivariant WF solution for a corner crack at a hole also involves several issues related to numerical integration and efficiency. A bivariant WF solution was originally released in NASGRO v5.0 as CC10. The range of geometries supported by CC10 aligned with the geometries in gas-turbine engines and, while the range of geometries was somewhat restricted, CC10 only required 72 reference solutions to calibrate the WF solution.

Verification

Recent advances in automation (discussed below) enable analysts to generate large sets of models economically. These capabilities have been employed to verify features of the existing solutions that were not possible previously. For example, earlier verification routines often reused the same geometries during verification that were used to calibrate a solution. The difference between the two analyses would

be the applied loadings to the verification tests. This approach would not test how the interpolation scheme predicted new geometries not employed during calibration.

A modern approach to verification is presented in Sobotka and McClung [13]. Here, the infinite set of geometric configurations supported by a SIF solution are sampled using Latin Hypercube Sampling [14], a space-filling design that bins the solution space based on the number of samples. This process results in a design of experiment (DOE) that is independent of the original DOE used to calibrate the solution. A series of relevant remote loadings and orthogonal stress gradients (applied to the crack faces) are selected as well to complete the DOE. SIF values in the DOE are then determined by finite element analyses as the baseline or actual SIF values (SIF^{FEA}) and using the practical SIF solution as the test value (SIF). Relative errors can then be computed as $RE (\%) = (SIF - SIF^{FEA})/SIF^{FEA} \times 100$, and these relative errors form a cumulative distribution of error if they are plotted as a rank ordering.

Figure 3 shows an example from this process. This result features SIF values computed at the a-tip for four different crack plane loadings given by P00 (uniform stress), P01 (linear stress in the c-tip direction), P10 (linear stress in the a-tip direction), and P11 (linear stress in both the a-tip and c-tip direction). The left-hand subplot shows the cumulative error plots from 500 geometries per loading condition for CC10. It has good accuracy given its age and number of reference solutions. However, the automation capability used to verify this geometry can also be used to generate a new set of reference solutions at limited cost. Consequently, we generated a larger set of reference solutions (748 vs. 72 for CC10 for the same geometric range) and defined the resulting bivariate WF SIF solution as CC26. This solution is shown on the right. More than 90% of CC26's solutions have less than 5% error. CC26 is slightly conservative with a median error value of 1%. A handful of solutions with errors >5% represent unusual combinations of crack shapes and sizes in plates with extreme values of thickness, hole size, and hole offset not likely to be encountered in practice. Note that while this approach to verification presumes errors, the variability measured in these solutions is much lower than the uncertainties associated with other inputs to the DT assessment, *e.g.*, the loading spectrum or crack growth rate.

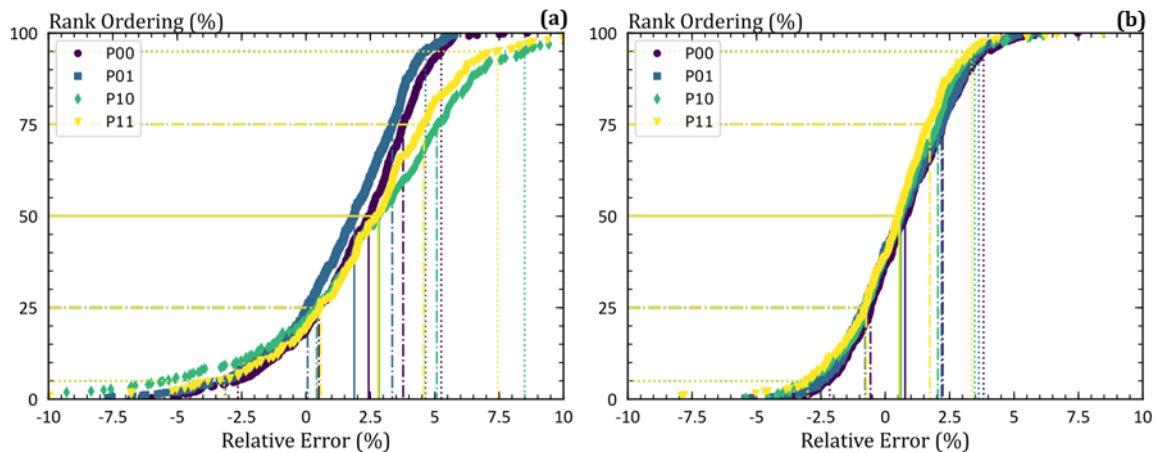


Figure 3: Verification plots for SIFs at the a-tip of CC10 (left) and CC26 (right).

COMPARISONS AND DISCUSSION

Thus far, we have mentioned five SIF solutions available in NASGRO for nominally the same geometry that is shown in Figure 1:

- CC02 – The classical Newman-Raju solution that is now “superseded”.
- CC16 – The Fawaz-Andersson solution with modified finite-width correction factors.
- CC08 – A univariate weight function solution.
- CC10 – A bivariate weight function solution with a small number of reference solutions.

- CC26 – A bivariate weight function solution with a larger number of reference solutions.

Without going into details, these solutions differ by more than their formulations and their pedigree. The most important features of a solution for practical analysis are the range of available geometries and the available loading conditions. Geometric limits may be restricted (CC02 and CC10) or expansive (CC08, CC16, and CC26). Loading conditions vary by solution. CC02 and CC16 only support S_0 , S_1 , and S_3 loading. CC08 directly supports S_0 , S_3 , and S_2 loading, with S_2 reflecting in-plane bending. CC26 directly supports all four remote loading conditions, whereas CC10 does not support any remote loading natively, though it may be supplied with the appropriate stress gradient. Furthermore, the WF solutions (CC08, CC10, and CC26) support local yielding and residual stresses.

These SIF solutions predict similar crack growth lives (within 2X of each other) in the following simple scenario as shown in Fig. 4. Here, the geometric ratios for the plate are set at $2B/W = 1$ (hole centered in plate), $D/2B = 0.25$, and $D/2t = 1, 2$, and 4, with one $D/2t$ per row in Figure 4. The thickness is fixed at 6.35 mm. The initial crack depth is $a = 0.127$ mm with $a = c$. FCG rates are defined using the NASGRO equation v4.0 set by material properties for 7075-T6 Plate material. The loadings have been generated using a constant amplitude spectrum with $R = 0.1$ and only one remote loading active per column. Figure 4 plots the crack depth (at the a -tip) and does not reflect the total predicted life that may be extended by a transition to a through crack solution. For this scenario, the various corner crack models generally reach consensus on the predicted life. Predicted lives converge as the plate becomes thinner (*i.e.*, $D/2t$ increases). The NR solutions (CC02) represent an outlier in the current predictions with more conservative life predictions for S_0 and S_3 loading. For out-of-plane bending (S_1), the bivariate WF solutions diverge from the data table solutions, perhaps due to the WF solutions picking up the negative stresses across the thickness. Of the solutions presented here, only CC26 supports all remote loading conditions, features an extensive geometry, supports shakedown, and enables residual stresses.

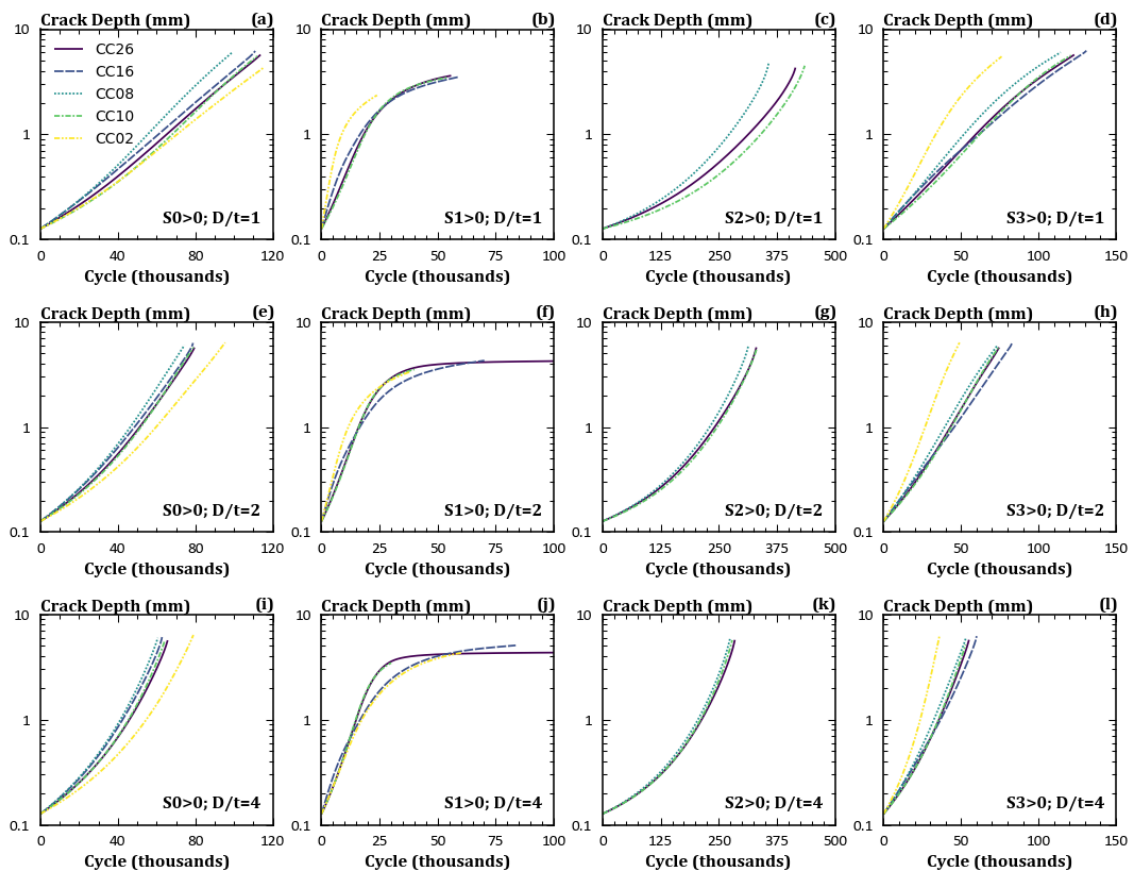


Figure 4: Life predictions showing the general agreement of five corner-crack SIF solutions.

GEOMETRIC VARIANTS

While the ideal geometry presented in Fig. 1 happens in practice, it is quite common for the idealized geometry to be combined with some additional feature. For example, multiple cracks may interact at the same hole and either increase or decrease FCG rates. In addition, a FCG assessment may result in crack transitions from corner cracks to through cracks. This section details these considerations and describes approaches to incorporate them into practical FCG assessments.

Multiple Cracks at One Hole

An earlier section mentioned the FA solution for two unequal cracks at a single hole and the large number of analyses required to support it. When this solution was implemented, it was noticed that some entries had unrealistic numbers that suggested data corruption. These entries were replaced using a scheme that replaced corrupt entries with entries that would be reproduced by interpolation using nearby entries. Practical analysis using this database required correction factors for finite-width plates and offset holes modified by an equivalent hole method (see the documentation of [1]).

To date, this solution represents one of the few solutions available for analysts to examine the impact of multi-site damage. Additional solutions have not been developed due to the excessive number of solutions that would be needed to populate the calibration matrix. Instead, analysts often need to rely on compounding approaches that approximate the unknown SIF values at multiple cracks using the known SIF values at similar geometries. Bombardier and Liao [15] provide one such solution for two unequal through cracks at a hole offset in a plate using a compounding method. The authors have extended the compounding approach [16,17] to more general problems as well.

Continuing Damage after Crack Transitions

Corner cracks transition to through cracks after one tip reaches the free surface, *i.e.*, $a \rightarrow t$. The exact depth at which crack transitions differs from one solution to another, with typical transition limits being between 90-99% of the thickness. Solutions with different transition criteria often have similar overall lives since the crack usually spends few cycles once the crack depth is on par with the thickness.

After the crack transitions, the new solution typically enforces a straight crack front for the remainder of the analysis. This approach limits the available loading scenarios that can be considered since out-of-plane bending could induce a curved crack front and different SIF values at the front surface and back surface. Early through crack solutions adopt a simple (though perhaps too simple) fix of approximating the driving force for the out-of-plane bending by applying half the value of the SIF solution for uniform tension. This ad-hoc approach lacks a physical basis. More recent developments enable curved-through crack fronts that permit a realistic evolution of the crack front under out-of-plane bending.

There are several available transition paths for multi-site damage for corner cracks at a hole. If both corner cracks break through the back face at the same instant, then the Bombardier and Liao solution [15] provides a reasonable transition path. It is more likely that the primary crack will break through the thickness before the secondary crack, and this scenario results in a hybrid crack geometry with a corner crack and a through crack. Again, a compounding solution represents a viable approach. Finally, the through crack could break through a ligament, resulting in a single corner crack once again. This scenario can be treated by combining the relevant stresses with a WF solution corrected for the effective sectional width. Here, new stresses on the single ligament must be computed due to load redistribution.

Countersunk Holes

Countersunk holes remove material from the outer face of the plate to form a conical entry so that a fastener head lies flush against the plate. Cracks may develop at either the faying surface or at the knee of the countersink. The countersunk hole alters the driving forces for crack growth and changes the

transition path since a crack may encounter multiple combinations of the countersunk hole itself, the straight bore, and the free surface. The countersunk angle varies for different applications.

Cronenberger [18] provides a SIF solution for a countersunk hole if the hole is far from all other boundaries. It only supports remote uniform tension. Crack tips are located on the knee and on the countersunk hole, or the crack tips can be located at one free surface and on the countersunk hole. The countersunk angle is fixed at 100° . This solution may extend other solutions with compounding.

Rows of Holes

Rows of holes are quite common in aerospace applications. For small cracks, small holes, and holes spaced far apart, the geometry shown in Fig. 1 results in SIF values that are essentially identical to the SIF values in a row of holes. Compounding methods could be used to approximate a SIF solution using a corner crack solution and a solution for a through crack at a row of holes. This method may have difficulties approximating the SIF at the a -tip.

Recently, an alternative solution was generated using new finite element analyses of a 3D corner crack at a hole in a row of holes. It supports the three loading configurations shown in Fig. 1 and supports three crack cases: two identical cracks at every hole; two identical cracks at one hole; and one crack at one hole. The new solution uses a Gaussian Process (GP) model (described later in this work) to interpolate between known solution values. This approach simplifies model development and reduces the computational effort that would be needed either to perform a full-factorial DOE or to produce a WF solution from scratch. Ongoing efforts are generating a curved-through crack solution to accompany the corner crack solution post-transition.

Pin Loading and Interference Fit

For S_3 loading, most SIF solutions feature a neat-fit pin inserted into a hole. Classical solutions often impose a wedge opening traction on the hole, with the traction defined based on an assumed pressure distribution. Using this approach, quarter-symmetric models may be used to generate a new SIF solution and to avoid the computational burden of contact iterations. However, various studies [19] show that if the pin is modelled as a deformable body, then the traction distribution is a function of the hole size and the friction coefficient. Consequently, CC08 and CC26 employ a solution stress computed using a deformable pin in contact with a deformable plate. The friction coefficient is set at a constant value of 0.3, despite its probable variation from this assumed value due to environmental, material, and wear during loading. Unfortunately, the actual value of the friction coefficient is not well characterized and not measured during loading. It should also be noted that SIF solutions are generally produced for open-hole configurations except when generating SIF solutions for pin-loading. Investigations by [20] indicate that this approach may be somewhat conservative.

In most SIF solutions with pin loading, increasing the pin loading results in a corresponding linear increase in the SIF solution. Recent investigations [1] demonstrate that the SIF solution depends on the magnitude of the applied loading for an interference-fit pin condition. These studies indicate that inputting residual stresses from the interference fit to a WF solution does not result in an accurate SIF solution. There is a nonlinear response at higher magnitudes of remote loading that pull the pin surface from the hole. Instead, a nonlinear SIF solution was developed that modifies the SIF value based on the associated loading magnitude. This solution is limited to a through crack and to loading combinations that do not generate significant plasticity.

Lugs

Lugs are almost always unique geometries, and at least one designer has made the offhand remark that, "Every lug is a unicorn." It can prove difficult to parameterize a lug for a SIF solution as a result. Previous solutions limited lugs to a straight, short geometry under vertical loading. Recently, new lug solutions [21] have been developed for an obliquely loaded and tapered lug with a variable height. These

solutions support corner cracks and through cracks. The crack location is based on maximum stress criteria (either the Mises stress or the maximum principal stress) and if the crack is positioned on a short ligament or long ligament. These lug solutions are based on modifications of the univariant WF solutions and feature stresses extracted at the appropriate angles.

STATE OF THE ART TECHNIQUES

Recent techniques have supported the development of new SIF solutions for corner cracks at holes. These techniques reduce the level of effort needed to build a solution and to reduce the data that needs to be stored for a solution. These capabilities have resulted in a significant increase in the number and fidelity of new SIF solutions. These also permit confidence to be built in these solutions through formal verification techniques that quantify the errors inherent in any practical SIF solution.

Nonlinear Interpolation by Gaussian Process Models

As the geometric complexity increases, there is a corresponding increase in the number of non-dimensional parameters that make new solutions intractable using spline functions constructed from a full factorial DOE. Consider a full factorial DOE with (arbitrarily) 10 geometries per non-dimensional parameter n . The number of finite element analyses needed to develop a new solution is then 10^n . Furthermore, many of these solutions are placed on the boundaries of the non-dimensional geometric range that are rarely used in an analysis.

GP models [22] provide an alternative approach to interpolation that reduces the number of required solutions. GP models are calibrated to minimize the uncertainty between the function and “training data” (*i.e.*, reference solutions) that are irregularly spaced, often based on a DOE generated by LHS. One common model used in some solutions discussed here may be written as shown in Eqn. (4):

$$g(x_1, x_2, \dots, x_n) = p_0 + \sum_{i=1}^n p_i x_i + \sum_{i=1}^N r_i \times \exp\left(-\sum_{j=1}^n \left(\frac{x_j - X_{ij}}{\lambda_j}\right)^2\right) \quad (4)$$

Eqn. (4) is a general expression with the following inputs and static defined quantities:

- n sets the number of non-dimensional geometric parameters;
- x_i represents an input non-dimensional geometric parameter, *e.g.*, $D/2t$;
- N denotes the number of training points in the model;
- X_{ij} defines a non-dimensional geometric parameter value for one training point;
- r_i reflects the residual values at the training points;
- p_i and λ_j indicate calibrated regression terms.

GP models are a class of machine-learning algorithms that have several attractive features. For our analyses, geometry correction factors defined by GP models require approximately at least 10X fewer finite element analyses to achieve a similar level of accuracy that is found in solutions built using spline functions. These models also feature a measure of uncertainty that can be used to improve their fit in relevant locations. The major drawback of GP models is that these models have more curvature than splines in regions with limited amounts of calibration data. Consequently, these models may require more investigation to ensure proper physical behaviour than associated models built with splines.

Principal Component Analysis

Principal Component Analysis (PCA) [23] decomposes a vector into orthogonal components that can be reconstructed to form the original vector. Furthermore, this PCA process ranks the orthogonal components by their contribution to variation of the original vector. Consequently, all PCA components

do not need to be stored to produce a reasonable approximation of the original vector. In very recent efforts, we have combined the GP models described above with PCA orthogonal components to predict the variation of bivariate stress fields near holes as a function of remote loading and geometry:

$$\sigma(\xi_i, \eta_j, x_1, x_2, \dots, x_n) = \mu(\xi_i, \eta_j) + \sum_{k=1}^m U_k(\xi_i, \eta_j) \times g_k(x_1, x_2, \dots, x_n) \quad (5)$$

Eqn. (5) features the following terms:

- ξ_i and η_j are the i^{th} and j^{th} points in a non-dimensional 2D grid of the ligament;
- x_i represents an input non-dimensional geometric parameter, *e.g.*, $D/2t$;
- $\mu(\xi_i, \eta_j)$ reflects the mean value of σ at point (ξ_i, η_j) ;
- m indicates the number of principal components used in the solution;
- $U_k(\xi_i, \eta_j)$ indicates the k^{th} orthogonal component from PCA at point (ξ_i, η_j) ;
- g_k denotes a GP model that provides the contribution to the stress for the k^{th} orthogonal component given the input non-dimensional geometric parameters.

Early estimates of the database needed to store data for a bivariate stress function suitable for spline interpolation indicated that the memory size would exceed the current NASGRO executable. The PCA approach outlined here enables the generation of a bivariate stress solution that requires similar storage as the univariate stress solution. This new capability has been incorporated into CC26. It may be useful to store and process a variety of multi-dimensional data beyond stresses in the future.

Automation

Techniques using GP models and PCA rely on the generation of large databases to identify statistical trends and to fit appropriate models. This data is most readily generated by automating the creation, execution, and post-processing of finite element analyses. While earlier solutions (*i.e.*, the FA solutions) invoked automation procedures to build large databases of models, developing these capabilities represented a significant burden. First, the meshing capabilities may have required direct intervention on the part of the users. Second, the computational constraints at the time limited the degrees of freedom that could be used in an analysis and necessitated detailed convergence studies for each geometry.

In recent years, the scripting capabilities supported by Abaqus, ANSYS, and StressCheck have become robust enough to support a variety of models appropriate for SIF calculations [24]. For example, Abaqus features a Python scripting capability that permits users to define a CAD model, assign material properties, build an assembly, define load steps, assign contact conditions, assign boundary conditions, mesh a 3D crack front, execute the analysis, and extract the SIF values across the crack front. This process requires only a few thousand lines of Python code, much of which is reusable for subsequent analyses. This capability was unavailable in the earlier eras.

Furthermore, computational capabilities available to engineers at large institutions enable analysts to execute linear-elastic models with 10^6 - 10^7 degrees of freedom without any hesitation. These models are 100X-1000X larger than the largest model used to generate the solutions for the NR solution and roughly 10X-100X larger than the largest models used to generate the FA solutions. Consequently, engineers can focus on fine-tuning their analysis procedure rather than focus excessively on convergence.

SUMMARY, DISCUSSION, AND FUTURE AREAS OF RESEARCH

This paper surveys SIF solutions for corner cracks at holes in plates. We have focused on the idealized geometry in Fig. 1 originally proposed by Newman and Raju. This geometry has been of perpetual interest to damage tolerance analysts due to its wide applicability to fracture critical locations. Newman and Raju produced the first SIF solution for this geometry, and it may represent the most widely used

SIF solution in practice. Fawaz and Andersson extended their solution by developing a large database of SIF solutions. Both sets of these classical solutions require a finite-width correction factor to support practical DT assessments. Alternatively, weight function solutions provide a method to support arbitrary loadings on the crack plane, and the structure inherent in weight function solutions means that they require many fewer analyses to calibrate than large databases. Weight function solutions have been developed for both univariant and bivariate stress fields that permit analysts to investigate the impact of local plasticity, residual stresses, and various remote loading conditions. While these different solutions have different formulations, pedigrees, and capabilities, results shown here suggest that modern solutions predict lives within 2X of the average value. Given these results, we recommend that the new bivariate weight function solution CC26 be considered as a new standard solution for predicting crack growth lives.

This work also documents geometries and loading conditions not explicitly covered by the idealized geometry with a single corner crack at a straight-bore hole with a neat-fit pin: holes with multiple corner cracks, hybrid transition solutions, countersunk holes, rows of holes, interference fit pins, and lugs. These common scenarios can be treated by recent SIF solutions with powerful, but incomplete capabilities, that can be extended through compounding approaches. We also discuss recent techniques that have permitted new solutions and promise to assist new advances in the future: Gaussian Process models; Principal Component Analysis; and rapid automation using commercial simulation software.

Over the past forty years, DT assessments have benefited from the efforts of various researchers to refine SIF solutions for corner cracks at holes in plates. These efforts have resulted in robust, efficient solutions with capabilities that exceed the capabilities of the original Newman-Raju classical solutions. The next generation of SIF solutions will need to expand these capabilities to consider persistent issues that, until recently, may have been neglected for more urgent concerns:

- Expand weight function methods to treat novel geometries.
- Increase compounding capabilities to approximate various geometries for design.
- Treat multiple cracks at holes in plates using the same rigor as single cracks at holes.
- Enable robust crack transition routes that consider all pertinent features, with a specific focus on treating through cracks subjected to out-of-plane bending.
- Provide solutions for countersunk hole geometries and the associated crack configurations.
- Consider the impact of rows and columns of holes upon SIF solutions.
- Evaluate how a filled hole impacts SIF solutions that are now treated as open holes.
- Add out-of-plane pin loads to the suite of loading conditions.
- Develop practical engineering methods that treat the influence on interference-fit pins and clearance-fit pins on SIF solutions for corner cracks in linear-elastic materials.
- Increase the above capabilities to consider limited plasticity from an interference fit.
- Expand the flexibility of solutions to support the broad array of lug geometries.
- Quantify the uncertainty of a SIF solution by rigorous verification.
- Propagate uncertainties for the full DT analysis into risk assessments of components.
- Estimate residual stresses arising from cold-expansion processes using practical methods.
- Link credible fatigue crack growth solvers with advanced simulation tools to develop trusted DT assessment capabilities needed for unique geometries not treatable by standard solutions.
- Provide methods to treat multi-site damage through frameworks that enable n-DOF crack growth engines, compounding, and multiple-crack interaction/linking.

While considerable evolutionary improvements to corner crack solutions have been made over the years, the problem of a corner crack at a hole in a plate remains as an opportunity for additional research to address and advance applications for the more complicated issues outlined above. Advances in these areas promise to reduce conservatism without sacrificing safety, to expand the range of scenarios routinely treated in DT assessments, and to reduce the uncertainty inherent in approximate solutions. To this end, we will continue to advance state-of-the-art SIF solutions and to deploy them in NASGRO in support of practical DT assessments.

REFERENCES

- [1] “NASGRO® Fracture Mechanics and Fatigue Crack Growth Analysis Software,” v10.1, Southwest Research Institute and NASA Johnson Space Center, August 2022. (www.nasgro.swri.org).
- [2] Raju, I.S., and Newman, J.C., Jr., (1979), In: *ASTM STP-677*, American Society for Testing and Materials, pp. 411-430, DOI: 10.1520/STP34926S.
- [3] Fawaz, S.A., and Andersson, B., (2004), *Engineering Fracture Mechanics*, vol. 71, n. 9-10, pp. 1235-1254. DOI: 10.1016/S0013-7944(03)00207-8.
- [4] Shah, R.C., (1976), In: *ASTM STP-590*, American Standard for Testing and Materials, pp. 429-459, DOI: 10.1520/STP590-EB.
- [5] Newman, J.C., Jr. and Raju, I.S., (1986), In: *Computational Methods in the Mechanics of Fracture*, Elsevier Science Publishers, pp. 311–334.
- [6] Renaud, G., Liao, M., and Bombardier, Y., (2012) In: *53rd Proceedings of the AIAA/ASME/ASCE/AHS/ASC Structures, Structural Dynamics and Materials Conference*, AIAA, DOI: 10.2514/6.2012-1700.
- [7] Newman, J.C., Jr., (2018) In: *Proceedings of the 2018 AIAA/ASCE/AHS/ASC Structures, Structural Dynamics, and Materials Conference*, AIAA SciTech Forum, DOI: 10.2514/6.2018-1471.
- [8] Wu, X and Xu, W., (2022), *Weight Function Methods in Fracture Mechanics: Theory and Applications*, Springer, 1st Edition, DOI: 10.1007/978-981-16-8961-1.
- [9] Bueckner, H.F., (1970), *Zeitschrift fuer Angewandte Mathematik & Mechanik*, vol. 50, n. 9, pp. 529-46.
- [10] Rice, J.R., (1972), *International Journal of Solids and Structures*, vol. 8, n. 6, pp. 751-758, DOI: 10.1016/0020-7683(72)90040-6.
- [11] Shen, G., and Glinka, G., (1991), *Theoretical and Applied Fracture Mechanics*, vol 15, n. 3, pp. 237-245, DOI: 10.1016/0167-8442(91)90022-C.
- [12] Lee, Y.D., McClung, R.C., and Chell, G.G., (2008), *Fatigue and Fracture of Engineering Materials and Structures*, vol. 31, n. 11, pp. 1004-1016, DOI: 10.1111/j.1460-2695.2008.01292.x.
- [13] Sobotka, J.C., and McClung, R.C., (2019), *Journal of Verification, Validation, and Uncertainty Quantification*, vol. 4, n. 2, DOI: 10.1115/1.4044868.
- [14] Simpson, T.W., Lin, D.K.J., and Chen, W., (2001), *International Journal of Reliability and Application*, vol. 2, n. 3, pp. 209–240.
- [15] Bombardier, Y. and Liao, M., (2011), *Journal of Aircraft*, vol. 48, n. 3, pp. 910-918, DOI: 10.2514/1.C031127.
- [16] Liao, M., Bombardier, Y., Renaud, G., Bellinger, N., and Cheung, T. (2009). In: *ICAF 2009, Bridging the Gap between Theory and Operational Practice*, Springer, DOI:10.1007/978-90-481-2746-7_44.
- [17] Bombardier, Y., Liao, M., and Renaud, G. (2011). In: *ICAF 2011 Structural Integrity: Influence of Efficiency and Green Imperatives*, Springer, DOI:10.1007/978-94-007-1664-3_19.
- [18] J. O. Cronenberger, (2011), M.S. Thesis, The University of Texas at San Antonio.
- [19] Sobotka, J.C., and McClung, R.C., (2019), *Fatigue and Fracture of Engineering Materials and Structures*, vol. 43, n. 5, pp. 955-964, DOI: 10.1111/ffe.13171.
- [20] Evans, R., Clarke, A., Heller, M., and Stewart, R., (2014), *Engineering Fracture Mechanics*, vol. 131, pp. 570-586, DOI: 10.1016/j.engfracmech.2014.09.012.
- [21] Sobotka, J.C., Lee, Y.D., McClung, R.C., Cardinal, J., (2019), In: *ICAF 2019, Structural Integrity in the Age of Additive Manufacturing*, Springer, DOI: 0.1007/978-3-030-21503-3_40.
- [22] Rasmussen, C. E. and Williams, C. K. I., (2006), *Gaussian Processes for Machine Learning*, The MIT Press, DOI: 10.7551/mitpress/3206.001.0001.
- [23] Jolliffe, I.T., (2002), *Principals Component Analysis*, Springer, DOI: 10.1007/b98835.
- [24] Sobotka, J.C. and McClung, R.C., (2018), In: *Science in the Age of Experience*, Dassault Systèmes.